

1 **Title:** Failure of colonization following gut microbiota transfer exacerbates DSS-induced colitis

2

3 **Authors:** Kevin L. Gustafson^{1,2,4#}, Trevor R. Rodriguez^{1,2#}, Zachary L. McAdams^{1,3,4}, Lyndon M.
4 Coghill^{1,5}, Aaron C. Ericsson^{1,2,4,6,7 *}, Craig L. Franklin^{1,2,4,6 *}

5 ¹ Department of Veterinary Pathobiology, University of Missouri, Columbia, MO 65201, USA

6 ² Comparative Medicine Program, University of Missouri, Columbia, MO 65201, USA

7 ³ Molecular Pathogenesis and Therapeutics Program, University of Missouri, Columbia, MO,
8 65201, USA

9 ⁴ MU Mutant Mouse Resource and Research Center, University of Missouri, Columbia, MO 65201,
10 USA

11 ⁵ University of Missouri Bioinformatics and Analytics Core, University of Missouri, Columbia, MO,
12 65211, USA

13 ⁶ University of Missouri College of Veterinary Medicine, Columbia, Missouri, MO 65201, USA

14 ⁷ University of Missouri Metagenomics Center, Columbia, Missouri, MO 65201, USA

15 # Authors contributed equally to this study

16 * Co-corresponding authors: Dr. Aaron Ericsson, ericssona@missouri.edu, Dr. Craig Franklin,
17 franklinc@missouri.edu

18

19

20

21

22

23

24 **Abstract**

25 To study the impact of differing specific pathogen-free gut microbiomes (GMs) on a murine model
26 of inflammatory bowel disease, selected GMs were transferred using embryo transfer (ET), cross-
27 fostering (CF), and co-housing (CH). Prior work showed that the GM transfer method and the
28 microbial composition of donor and recipient GMs can influence microbial colonization and
29 disease phenotypes in dextran sodium sulfate-induced colitis. When a low richness GM was
30 transferred to a recipient with a high richness GM via CH, the donor GM failed to successfully
31 colonize, and a more severe disease phenotype resulted when compared to ET or CF, where
32 colonization was successful. By comparing CH and gastric gavage for fecal material transfer, we
33 isolated the microbial component of this effect and determined that differences in disease severity
34 and survival were associated with microbial factors rather than the transfer method itself. Mice
35 receiving a low richness GM via CH and gastric gavage exhibited greater disease severity and
36 higher expression of pro-inflammatory immune mediators compared to those receiving a high
37 richness GM. This study provides valuable insights into the role of GM composition and
38 colonization in disease modulation.

39

40 **Key Words:** Gut microbiota transfer, DSS-induced colitis, Microbiome colonization efficiency,
41 Inflammatory bowel disease (IBD), Fecal microbiota transfer (FMT)

42

43 **Introduction**

44 The gut microbiome (GM), the microorganisms that inhabit the gastrointestinal tract of humans
45 and animals, plays an important role in health and disease pathogenesis and severity^{1,2}. Common
46 diseases that may be influenced by features within the GM include inflammatory bowel disease
47 (IBD)³, colon cancer⁴, and autism⁵ among others. In the case of IBD, changes in the GM

48 characterized by reduced richness of symbiotic commensals (i.e., dysbiosis) may exacerbate
49 inflammation⁶. This dysbiosis induces further immune reactions and inflammation characterized
50 by the production of immune mediators, reactive oxygen species, and antimicrobial peptides when
51 pathobiont microbes breach the mucosa^{7,8}. While the GM plays an important role in both
52 physiology and pathophysiology of many diseases including IBD, studying the GM in humans can
53 be cumbersome and difficult due to varying backgrounds of individuals, unknown genetic
54 contribution to disease⁹ and the correlative nature of human studies. To overcome these
55 challenges, animal models have been established to answer questions concerning how the
56 microbiome interacts with and influences the health of the host. Studies performed in gnotobiotic
57 and germ-free rodents have established the need for a healthy GM for proper biological
58 development and physiology of the host organism¹⁰⁻¹². While animal models are essential to the
59 advancement of scientific knowledge, many studies utilizing rodents as models suffer from poor
60 reproducibility or translatability^{13,14}. Awareness of these issues has led the National Institutes of
61 Health to launch an initiative to improve the translatability and reproducibility in research to make
62 more investigators and their laboratories aware of the need to improve scientific rigor¹⁵.

63 The composition of the GM has an impact on the disease state of the rodent host¹⁶⁻¹⁹. The rodents
64 provided to the research community by the largest suppliers are colonized by GMs that
65 significantly differ in alpha and beta-diversity^{20,21}. Furthermore, research performed in isogenic
66 mice where the experimental groups harbor these different supplier-origin GMs have shown that
67 the GM can influence disease severity independent of genetic contributions in a chronic dextran-
68 sodium sulfate (DSS) -induced murine model of IBD²². Previous work in our lab has shown that
69 when co-housing is used to transfer a complex GM, colonization by the donated GM is less
70 successful and may result in severe DSS-induced disease and mortality. We sought to replicate
71 these findings in an acute model of DSS colitis and confirm that the effect on disease severity is
72 attributable to the GM and not an unexplained factor of the co-housing method. We leveraged the

73 differences in GM alpha and beta diversity between a Jackson Laboratory-origin GM, and Envigo-
74 origin GM²³. Specifically, we hypothesized that the transfer of donor microbiome to recipients
75 naturally during the post-partum period (i.e., via embryo transfer (ET) of recipient germplasm in
76 surrogate dams harboring the donor GM) or within the first 24 hours of life (i.e., via cross-foster
77 (CF) of recipient pups on surrogate dam donors) would result in more complete colonization of
78 the donor GM than co-housing for one month beginning at weaning.

79 We also hypothesized that attempts to transfer a comparably low-richness GM to recipients
80 harboring a high-richness GM via CH would result in particularly low transfer efficacy, and the
81 most severe disease when challenged with DSS at seven weeks of age. During the CH process,
82 donor and recipient mice were grouped together at weaning (21 days) in cages containing two
83 donors and two recipients, a procedure that could produce inadvertent effects on recipient mice
84 via psychosocial stressors or other unknown factors. To obviate any potential effects of physical
85 contact between the donor and recipient mice during the CH procedure, we included additional
86 treatments groups with the same timing and donor and recipient GMs, wherein the GM was
87 transferred via weekly gastric gavage and dirty bedding transfer. Recipient mice receiving the
88 reciprocal GM via ET, CF, CH, or gastric gavage and transfer of dirty donor bedding (GA) were
89 challenged with a single cycle of DSS, followed by assessment of disease severity via weight loss
90 and mortality, histological examination, colon length at necropsy, and production of inflammatory
91 mediators. Supporting a primary influence of poorly colonizing microbes rather than factors
92 associated with direct physical contact between donors and recipients, we hypothesized that mice
93 receiving a low-richness GM via GA and CH would have equivalent, severe DSS-induced disease
94 compared to all other groups. Conversely, if mice receiving the low-richness GM via CH
95 developed more severe disease than mice receiving the same GM via GA, it would indicate
96 differences in disease severity and survival are associated at least in part with physical contact
97 between recipients and donors.

98

99 **Methods**

100 **Ethics Statement**

101 All activities and experiments described using animal models were performed in accordance with
102 the Guide for the Care and Use of Laboratory Animals, and the Institutional Animal Care and Use
103 Committee of the University of Missouri, an AAALAC-accredited institution, approved all animal
104 use procedures (MU IACUC protocols 9587 and 36781).

105 **Mice**

106 C57BL/6J (B6J) and C57BL/6NHsD (B6N) mice were procured directly from The Jackson
107 Laboratory (Bar Harbor, ME) or Envigo (now Inotiv, Indianapolis, IN), respectively, and bred to
108 produce GM recipient mice. Embryo transfer, cross-fostering, and co-housing transfer methods
109 were performed as previously described²². Colonies of mice were housed under barrier conditions
110 in microisolator cages with compressed pelleted paper bedding and nestlets, on ventilated racks
111 with *ad libitum* access to 5053 (LabDiet, St. Louis, MO) rodent chow and acidified, autoclaved
112 water. Mice were housed under a 12:12 light/dark cycle. Mice were determined to be free of
113 bacterial pathogens including *Bordetella bronchiseptica*, *Filobacterium rodentium*, *Citrobacter*
114 *rodentium*, *Clostridium piliforme*, *Corynebacterium bovis*, *Corynebacterium kutscheri*,
115 *Helicobacter* spp., *Mycoplasma* spp., *Rodentibacter* spp., *Pneumocystis carinii*, *Salmonella* spp.,
116 *Streptobacillus moniliformis*, *Streptococcus pneumoniae*; adventitious viruses including H1,
117 Hantaan, KRV, LCMV, MAD1, MHV, MNV, PVM, RCV/SDAV, REO3, RMV, RPV, RTV, and
118 Sendai viruses; intestinal protozoa including *Spironucleus muris*, *Giardia muris*, *Entamoeba*
119 *muris*, trichomonads, and other intestinal flagellates; intestinal helminths including pinworms and
120 tapeworms; and external parasites including all species of lice and mites, via quarterly sentinel
121 testing.

122 *CD-1 donor mice.* All CD-1 mice that were used as donors were from two colonies in which the
123 founders were originally purchased from Charles River (CrI:CD1(ICR), Frederick, MD), and were
124 generated via rederivation to harbor either a high richness Envigo origin GM (GM^{High}), or a low
125 richness Jackson Laboratory origin GM (GM^{Low}) as previously described²⁴. All donor mice were
126 reared at the authors' institution and the two colonies have been maintained and continually
127 monitored for GM stability within our facility for over 35 generations. Additionally, a rotational
128 breeding scheme and routine introduction of CD-1 genetics via embryo transfer from CD-1 mice
129 purchased from Charles River allows for the maintenance of allelic heterozygosity within each
130 colony and ensures these colonies do not become genetically distinct from each other. Since CD-
131 1 mice that harbor a Jackson Laboratory origin GM were found to have a GM with low
132 phylogenetic richness and diversity, the GM of these mice was designated GM^{Low}. Similarly, since
133 CD-1 mice that harbored an Envigo origin GM were found to have a GM with high phylogenetic
134 richness and diversity relative to GM^{Low}, the GM of these mice was designated GM^{High}.

135 *Embryo transfer.* ET was performed at the authors' institution as previously described²³. Briefly,
136 B6J and B6N mice were obtained directly from respective producers, bred, and embryos were
137 collected at the two-cell stage. Embryos were surgically transplanted into GM donor
138 pseudopregnant CD-1 surrogate dams. GM donor surrogate CD-1 mice were allowed to give birth
139 and rear the pups (**Sup Fig S1A,B**). Pups that were generated via ET were then bred together to
140 generate a second generation to simulate the breeding that is sometimes necessary to obtain
141 enough animals to power scientific experiments due to low animal yields from embryo transfer
142 procedures²⁵. Numbers obtained from these breedings are as follows: GM^{High}ET ($n = 12/\text{sex}$),
143 GM^{Low}ET ($n = 12/\text{sex}$). Both male and female mice were included in the ET groups at a 1:1 ratio.

144 *Cross-fostering.* B6J and B6N mice, obtained directly from respective producers, were bred to
145 generate GM recipient mice. CD-1 dams were time-mated simultaneously with the B6J and B6N
146 dams to act as cross-foster surrogate dams. B6J and B6N pups were cross-fostered to a CD-1

147 GM donor dam harboring high richness GM^{High} or low richness GM^{Low}, respectively, within 12
148 hours following birth (**Sup Fig S1C,D**). Numbers obtained from the cross-fostering procedure are
149 as follows: GM^{High}CF ($n = 12$ males, 11 females), GM^{Low}CF ($n = 12$ /sex). To limit the possibility of
150 cannibalism and help facilitate GM transfer, 2-3 CD-1 pups born to the surrogate dams remained
151 within the litters.

152 *Co-housing*. B6J and B6N mice, obtained directly from respective producers, were bred to
153 generate GM recipient mice. CD-1 dams were time-mated simultaneously with the B6J and B6N
154 dams to generate GM donor mice. At 21 days of age, recipient B6J and B6N mice were weaned
155 and co-housed with weanling CD-1 mice harboring GM^{High} or GM^{Low}, respectively (**Sup Fig S1E-**
156 **H**). B6 mice were co-housed with age- and sex-matched CD-1 donors at a 1:1 ratio. Numbers
157 obtained from the co-housing procedure were as follows for the first experiment: GM^{High}CH ($n =$
158 12 /sex), GM^{Low}CH ($n = 12$ /sex). For the second experiment: GM^{High}CH ($n = 7$ males, 8 females),
159 GM^{Low}CH ($n = 8$ males, 8 females).

160 *Gastric gavage (GA)*. B6J and B6N mice, obtained directly from respective producers, were bred
161 to generate GM recipient mice. At weaning, mice were placed into cages with littermates of the
162 same sex. Following weaning, mice were exposed to the reciprocal GM by gastric gavage of 0.2
163 mL of fecal slurry once per week prepared from feces of age- and sex-matched CD-1 donor mice,
164 and transfer of dirty bedding from cages of age- and sex-matched CD-1 donor mice three times
165 per week up to seven weeks of age (**Sup Fig S1I,J**). The fecal slurry was prepared by collecting
166 a fecal sample from respective CD-1 donor mice. For each sample, 1 mL of 1X PBS was added
167 to a 2 mL microcentrifuge tube containing a 5 mm steel ball and an approximately 5 mm portion
168 of the donor fecal pellet. The fecal sample was homogenized in a Qiagen Tissuelyser 2.0 for 30
169 seconds at 30 Hz to create a fecal slurry. Following homogenization, all samples were pooled
170 within their respective GM by passing the individual slurry samples through a 70 μ m nylon mesh
171 filter into the same 50 mL conical tube. Numbers obtained for the gastric gavage groups in the

172 second experiment were as follows: GM^{High}GA ($n = 6$ males, 7 females), GM^{Low}GA ($n = 7$ males,
173 6 females).

174 **Fecal sample collection**

175 Antemortem fecal samples were collected by placing mice in a sterile autoclaved empty cage and
176 allowing them to defecate 2-3 fecal pellets which were promptly collected and stored at -80°C until
177 DNA extraction was performed. Feces were collected from pregnant GM donor CD-1 mice on day
178 18 of gestation to limit the incidence of cannibalism of the pups. GM recipient mouse fecal
179 samples were collected at three and seven weeks of age.

180 **Dextran sodium sulfate administration**

181 At seven weeks of age, all recipient mice were administered freshly reconstituted dextran sodium
182 sulfate (DSS) at a concentration of 2.5% in drinking water for seven days, followed by seven days
183 of DSS-free standard autoclaved drinking water. Mice were weighed daily during the seven days
184 of DSS administration and the following seven days after discontinuing DSS to monitor weight
185 loss, with exception of the GM^{High}CF cohort where the first- and third-day's weights during DSS
186 administration were inadvertently not recorded. At the end of the 14 days, mice were humanely
187 euthanized, and samples collected. Per the IACUC protocol humane endpoints, any mice that
188 lost greater than or equal to 20% of their pre-DSS administration weight, or were assessed by the
189 investigators to be moribund, were humanely euthanized and samples immediately collected.

190 **Necropsy**

191 At nine weeks of age, all DSS-treated mice were humanely euthanized by CO_2 asphyxiation,
192 followed by cervical dislocation according to the AVMA guidelines on humane euthanasia.
193 Immediately following euthanasia, the cecum and colon were removed, and colon lengths were
194 measured from the cecocolic junction to the rectum. The most distal fecal pellets within the colon
195 were collected and promptly stored at -80°C . For the first experiment, cecum and colons were

196 flushed, placed into cassettes, and immersed in 10% neutral buffered formalin to fix for
197 histological slide preparation. For the second experiment, the colon was incised longitudinally and
198 flattened on card stock, serosal side down. Tissue was then bisected longitudinally and one half
199 of the full length was immersion fixed in formalin while the other half was placed in a 2 mL
200 microcentrifuge tube, flash frozen in liquid nitrogen, and promptly stored at -80°C until protein
201 extraction was performed for immune mediator analysis.

202 **Microbiome analysis**

203 *DNA extraction.* DNA from fecal samples was extracted using the QIAamp PowerFecal DNA kit
204 (Qiagen) per manufacturer instructions, with the exception that homogenization was performed in
205 a 2 mL microcentrifuge tube containing a 5 mm steel ball and placed in a Qiagen TissueLyser 2.0
206 at 30 Hz for 10 minutes. All other steps were performed per the manufacturer instructions. DNA
207 concentration was quantified using the Qubit® 2.0 Fluorometer with the Qubit dsDNA BR assay
208 (Invitrogen) following manufacturer's protocol.

209 *16S rRNA amplicon library preparation and sequencing.* Extracted fecal DNA was processed at
210 the University of Missouri Genomics Technology Core Facility. Bacterial 16S rRNA amplicons
211 were constructed via amplification of the V4 region of the 16S rRNA gene using previously
212 developed universal primers (U515F/806R), flanked by Illumina standard adapter sequences^{26,27}.
213 Oligonucleotide sequences are available at proBase²⁸. Dual-indexed forward and reverse primers
214 were used in all reactions. PCR was performed in 50 µL reactions containing 100 ng
215 metagenomic DNA, primers (0.2 µM each), dNTPs (200 µM each), and Phusion high-fidelity DNA
216 polymerase (1U, Thermo Fisher). Amplification parameters were 98°C^(3 min) + [98°C^(15 sec) + 50°C⁽³⁰
217 ^{sec)} + 72°C^(30 sec)] × 25 cycles + 72°C^(7 min). Amplicon pools (5 µL/reaction) were combined,
218 thoroughly mixed, and then purified by addition of Axygen Axyprep MagPCR clean-up beads to
219 an equal volume of 50 µL of amplicons and incubated for 15 minutes at room temperature.
220 Products were washed multiple times with 80% ethanol and the dried pellet was resuspended in

221 32.5 µL EB buffer (Qiagen), incubated for two minutes at room temperature, and then placed on
222 a magnetic stand for five minutes. The final amplicon pool was evaluated using the Advanced
223 Analytical Fragment Analyzer automated electrophoresis system, quantified using quant-iT HS
224 dsDNA reagent kits, and diluted according to Illumina's standard protocol for sequencing on the
225 MiSeq instrument.

226 *Bioinformatics*. Primers were designed to match the 5' ends of the forward and reverse reads.
227 Cutadapt²⁹ (version 2.6) was used to remove the primer from the 5' end of the forward read. If
228 found, the reverse complement of the primer to the reverse read was then removed from the
229 forward read as were all bases downstream. Thus, a forward read could be trimmed at both ends
230 if the insert was shorter than the amplicon length. The same approach was used on the reverse
231 read, but with the primers in the opposite roles. Read pairs were rejected if one read or the other
232 did not match a 5' primer, and an error-rate of 0.1 was allowed. Two passes were made over each
233 read to ensure removal of the second primer. A minimal overlap of three bp with the 3' end of the
234 primer sequence was required for removal. The QIIME2³⁰ DADA2³¹ plugin (version 1.10.0) was
235 used to denoise, de-replicate, and count ASVs (amplicon sequence variants), incorporating the
236 following parameters: 1) forward and reverse reads were truncated to 150 bases, 2) forward and
237 reverse reads with number of expected errors higher than 2.0 were discarded, and 3) Chimeras
238 were detected using the "consensus" method and removed.

239 **Tissue histological examination and scoring.**

240 Cecum and colon were trimmed, embedded, and sectioned by the histology services of IDEXX
241 BioAnalytics (Columbia, MO). Histological examination was performed by two blinded laboratory
242 animal veterinarians experienced in reviewing GI tissues (KG and TR). Slides were randomly
243 ordered so that reviewers were blinded to transfer method, transfer direction, and sex. Reviewers
244 assigned a lesion score based on the degree of inflammation and epithelial changes, and overall
245 percentage of the colonic lesions (**Sup Table S1**). Scores that differed by 1 between reviewers

246 were averaged. When scores differed by greater than 1, reviewers re-examined slides together
247 and generated a consensus score. Only after agreement was reached on scores were reviewers
248 unblinded to treatment groups.

249 **Protein extraction and immune mediator analysis**

250 Colon tissue from six males and six females from each GM transfer group in the co-housing and
251 gavage groups were randomly selected for cytokine analysis. Protein was extracted from colon
252 tissue by adding 500 μ L of 1X phosphate-buffered saline to each colon tissue sample. Samples
253 were then homogenized in a 2 mL microcentrifuge tube containing a 5 mm-diameter steel ball.
254 Mechanical homogenization was performed using a Qiagen Tissuelyser 2.0 at a frequency of 30
255 Hz for 5 minutes. Samples were then centrifuged at 9,000 $\times g$ for 9 minutes and supernatant
256 collected. Protein concentrations were quantified using the Qubit® 2.0 Fluorometer with the Qubit
257 protein BR assay (Invitrogen) following the manufacturer instructions. Protein samples were
258 analyzed at a concentration of 300-550 μ g/mL using a ProcartaPlex™ Mouse Immune Monitoring
259 Panel 48-Plex kit (Invitrogen) according to manufacturer instructions. A standard curve was
260 generated using the standards provided and according to the manufacturer's protocol. All samples
261 were run in duplicate. Data was acquired on a routinely validated and calibrated Luminex xMAP
262 INTELLIFLEX system. Samples for which the immune mediator concentrations were too low to
263 be detected were designated to have a concentration of zero due to the high sensitivity and
264 specificity of the assay.

265 **Statistics**

266 Two-way permutational analysis of variance (PERMANOVA) was used to test for significant main
267 effects in beta diversity of transfer method and donor/recipient. Three-way PERMANOVA was
268 used to test for significant main effects in beta diversity of transfer method, transfer direction, and
269 donor/recipient, followed by one-way PERMANOVA for donor/recipient group pairwise
270 comparisons. One-way and Two-way PERMANOVA analysis was performed using PAST 4.09

271 software³² and was based on Jaccard dissimilarities. Three-way PERMANOVA testing was based
272 on Jaccard dissimilarities using the *adonis2* library from the *vegan* library³³. Distances between
273 group centroids were determined using the *usedist* library³⁴. Comparisons in percent weight
274 change were performed by calculating area under the curve (AUC) for each mouse from days 6
275 to 14 of DSS treatment when marked weight loss occurred, and normalizing AUC to days survived
276 to account for animals that were removed from the study during DSS treatment due to reaching
277 humane endpoints. For percent weight loss data in experiment 1, a one-way analysis of variance
278 (ANOVA) was used to test for effect of transfer method within the GM^{High} cohorts followed by
279 Tukey *post hoc* for pairwise comparisons. Due to lack of normality in the GM^{Low} cohorts, a Kruskal-
280 Wallis ANOVA on Ranks was used to test for effect of transfer method followed by Dunn's *post*
281 *hoc* for pairwise comparisons. A Student's t-test was used to test for significant differences
282 between the percent weight loss of GM^{High}CH and GM^{Low}CH. Due to lack of sufficient animals
283 remaining in the GM^{Low}CH cohort (two animals remained following day 10), statistical analysis of
284 the cohort percent weight loss was only performed to day 10 of DSS treatment. For percent weight
285 loss data in experiment 2, a two-way ANOVA was used to test for main effects of transfer method
286 and transfer direction followed by Tukey *post hoc* for pairwise comparisons. For unifactorial
287 survival data, a survival LogRank analysis was used to test for significant effects. For multifactorial
288 survival data, a Cox proportional hazards test was used to test for significant main effects in
289 disease survivability including transfer method, transfer direction, and sex. Three-way ANOVA
290 was used to test for significant main effects of transfer method, transfer direction, and sex for
291 Chao-1 richness, weaning and week seven weights, colon lengths, histological lesion scores, and
292 cytokine/chemokine concentrations followed by Tukey's *post hoc* analysis for pairwise
293 comparisons. Univariate data was first tested for normality using the Shapiro-Wilk method. All
294 univariate data analysis was performed using SigmaPlot 15.0 (Systat Software, Inc, San Jose,
295 CA). Due to lack of normality in the concentrations of MIP-2 α , IL-22, and IL-6 these data were
296 transformed prior to performing three-way ANOVA analysis. MIP-2 α concentrations were

297 normalized by square root transformation, and IL-22 and IL-6 concentrations were normalized by
298 logarithmic (log) transformation. Due to uniform lack of normality across immune mediator
299 concentrations, a Mann-Whitney U test was used to test for statistical differences in immune
300 mediator concentrations between GM^{High} and GM^{Low} treatment groups, as well as co-housing and
301 gavage treatment groups. All diversity and richness indices were calculated using PAST 4.09
302 software.

303

304 **Results**

305 **Efficiency of GM transfer is determined by transfer method**

306 We first sought to determine if we could replicate our previous findings²² in an acute DSS-colitis
307 disease model. To provide clarity regarding transfer terminology and nomenclature used in this
308 study, we have provided **Sup Fig S1** as a schematic to assist the reader in following the
309 experimental groups and transfer procedures. To be clear, all GM donor CD-1 mice used in this
310 study were from outbred colonies where the founders were originally purchased from Charles
311 River, and given their respective microbiomes via ET²⁴. To assess GM transfer efficiency, transfer
312 recipients receiving the respective GM via ET were compared to the CD-1 ET dams (i.e., the GM
313 donors in this case). Similarly, CF recipients were compared directly to their CF surrogate dams.
314 For CH, recipients were compared to feces from the dams of the CD-1 co-housing donors as the
315 GMs of the CD-1 donors housed with the B6 recipients would be modulated by the recipient B6
316 microbiome via mutual coprophagia. We performed 16S rRNA amplicon sequencing analysis on
317 feces from the recipient mice of the ET, CF, and CH groups at seven weeks of age, and compared
318 these to the respective donor fecal microbiome. To assess transfer efficiency, unweighted beta
319 diversity between donors and recipients was first examined. Principal coordinate analysis (PCoA)
320 revealed little separation between recipient and donors in the GM^{High}ET, CF, and CH groups, with
321 the GM^{High}CH group showing greater dissimilarity to their donors (Distance between centroids

322 [CD] = 0.500) compared with the ET (CD = 0.409) and CF (CD = 0.283) groups (**Figure 1a**). In
323 contrast, the GM^{Low}ET and CF groups showed similar composition to their donors (CD of 0.322
324 and 0.386, respectively), but the GM^{Low}CH group showed marked separation from their donors
325 (CD = 0.623) (**Figure 1b**). When beta diversity of all six transfer groups was compared, a stark
326 difference in beta diversity between the recipient and donors within the GM^{Low}CH group and the
327 other transfer groups became apparent by the greater separation of the GM^{Low}CH donors and
328 recipients (**Sup Fig S2; Sup Table S3**). When alpha-diversity was assessed, the GM^{High} recipients
329 showed no statistically significant differences in GM richness between the donor and recipient
330 GMs in any transfer method (**Figure 1c**). The GM^{Low}ET and CF groups showed no significant
331 differences between donor and recipient mice, but a marked significant difference was observed
332 in the GM^{Low}CH group with the recipient mice having a greater GM microbial richness compared
333 with the donors at seven weeks of age (**Figure 1d**) resulting in a pattern similar to what was
334 observed with beta diversity.

335 **Disease phenotype determined by efficiency of GM transfer**

336 *Weight loss.* While the GM^{High} groups showed a small but significant difference in weight loss
337 between the CF and CH groups (**Figure 2a**), the GM^{Low} cohorts showed a dramatic significant
338 difference in their weight loss between the three groups with CH have the most severe weight
339 loss (**Figure 2b**). Of note, while pre-DSS body weights collected at weaning revealed significant
340 differences between transfer method groups in both GM^{High} and GM^{Low} recipient mice (**Sup Figure**
341 **S3A-B**), those differences were normalized at seven weeks of age, the age when DSS
342 administration began, with no differences detected between groups (**Sup Fig 3C-D**). While CH
343 was clearly associated with more severe disease in GM^{Low}CH mice, GM^{High}CH mice developed
344 similar disease to GM^{High}ET and GM^{High}CF mice, suggesting that CH *per se* is not solely
345 responsible for the severe disease observed in GM^{Low}CH mice (**Sup Fig S4A-B**).

346 *Survival.* To assess whether the method and efficiency of GM transfer can influence disease
347 phenotype, a DSS colitis model was employed in which DSS was administered in the drinking
348 water for one week, followed by one week of recovery with untreated water. Immediate outcomes
349 measures including weight loss and survival demonstrated profound differences in co-housed
350 groups. No significant differences in experimental survival among the GM^{High} groups were
351 observed with only two individuals, one in the ET group and one in the CH group, requiring
352 euthanasia due to disease severity (**Figure 2c**). However, the GM^{Low}CH group had a significant
353 number of individuals (91.6%) requiring euthanasia due to weight loss and disease severity
354 (**Figure 2d**).

355 *Colon lengths and lesion scores.* Following euthanasia, colon length measurements revealed a
356 difference between the GM^{Low}CH group, GM^{Low}CF groups, and the four other groups (**Figure 2e**)
357 with GM^{Low} CH having the greatest reduction in colon length. To determine if the shorter colon
358 lengths in GM^{Low}CH mice were due to being euthanized before the two-week endpoint, colons of
359 mice taken down early were compared to those who continued to the end of study. Interestingly,
360 no difference was detected in colon length of those mice that were euthanized early compared
361 with those of the mice who survived to the end of study (**Sup Fig S5A**). Histological examination
362 also showed the GM^{Low}CH group had significantly greater disease with a majority of the lesions
363 characterized by severe colonic epithelial ulceration and erosion with marked immune cell
364 infiltration (**Figure 2f**), the most severe being in those mice that were euthanized early (**Sup Fig**
365 **S5B**).

366 **Co-housing disease phenotype is a result of the transferred GM and transfer efficiency**

367 With the interesting repeatable results obtained in the GM^{Low}CH group, we next wanted to confirm
368 that these observations were a result of the GM-associated microbial factors and not other factors
369 associated with CH. To this end, a second experiment was performed where GM^{High}CH and
370 GM^{Low}CH were compared to two groups in which the recipient mice were exposed to reciprocal

371 GMs via gastric gavage (GA) and dirty bedding transfer. Following four weeks of GM transfer via
372 CH or GA, sequencing of the fecal DNA showed that the effect of transfer direction was significant,
373 but not method of transfer, as no differences in microbial composition or richness were found
374 between the CH and GA treatment groups in either transfer direction (**Figure 3a-b**). Similar to
375 previous experiments, transfer of a high richness GM to a recipient harboring a low richness GM
376 resulted in more efficient colonization than transfer of a low richness GM to a recipient harboring
377 a high richness GM (**Sup Fig S6A-C**). When transferring a high richness GM to a low richness
378 recipient by CH or GA, the recipients shared similar GM composition across these transfer
379 methods (**Sup Fig S6A**), and while richness was significantly different, the CH and GA groups
380 had a greater microbial richness than the donors at week seven (**Sup Fig S6B**). In contrast, GM^{Low}
381 donors did not successfully transfer their GM composition or taxonomic richness to the B6N
382 recipients (**Sup Fig S6A,C**).

383 We next administered DSS to the four treatment groups with a single one-week pulse followed by
384 a week of recovery. A significant difference was observed between the mice receiving GM^{Low} or
385 GM^{High}, with transfer of a low richness GM to recipients harboring GM^{High} resulting in greater
386 weight loss (**Figure 3c**) and higher mortality (**Figure 3d**). However, these marked weight loss and
387 survival differences were not observed between the CH and GA groups within either transfer
388 direction. Similarly, analysis of colon lengths collected at necropsy showed a significant difference
389 between GM^{Low} and GM^{High} recipients, while transfer method had no effect within either GM
390 (**Figure 3e**). Colon tissue was also collected for histological examination, which revealed a similar
391 pattern where mice receiving GM^{Low} had significantly greater lesion severity than mice receiving
392 GM^{High}, regardless of transfer method (**Figure 3f**).

393 **Transfer of GM^{Low} to mice harboring GM^{High} results in increased immune mediators within**
394 **diseased colons**

395 Lastly, local immune responses were assessed using bead-based immunoassay quantification of
396 45 cytokines, chemokines, and other immune mediators. When concentrations were compared
397 based on the GM being transferred, nine inflammatory mediators were significantly elevated in
398 mice receiving GM^{Low} (**Figure 4a; Sup Table S4**). Alternatively, comparison based on transfer
399 method failed to detect a difference in any of the immune mediator concentrations (**Figure 4b;**
400 **Sup Table S5**), suggesting that the transfer efficiency, not transfer method, is driving the immune
401 response. Affected cytokines and chemokines included the chemokine MIP-2 α (**Figure 4c**)
402 involved in recruitment of innate immune cells in acute phase immune responses, IL-22 (**Figure**
403 **4d**) which promotes epithelial proliferation and regeneration in response to injury, and the pro-
404 inflammatory cytokine IL-6 (**Figure 4e**). Immune mediator group concentration means and
405 standard deviations are provided in **Sup Table S6**.

406

407 **Discussion**

408 In this study, we have leveraged an acute model of DSS colitis to elucidate the impact of gut
409 microbiota (GM) composition, richness and efficiency of transfer methods on disease phenotypes.
410 The results presented here confirm previous results that embryo transfer and cross-fostering
411 share similarly high transfer efficiency regardless of GM composition²². In contrast, co-housing at
412 weaning is less effective, suggesting that GM transfer early in life facilitates microbial colonization.
413 Furthermore, the relationship of the recipient and donor microbiome during co-housing
414 determines transfer efficiency. Differences between groups in disease severity suggest that the
415 efficiency of transfer influences the severity of weight loss, mortality, reduction in colon length,
416 and histological lesion severity, corroborating previous results using a chronic DSS colitis model²².
417 The addition of groups receiving GM transfer via gavage and dirty bedding provides further
418 evidence that the severity of colitis is negatively associated with the efficacy of GM colonization
419 following transfer.

420 During the colonic epithelial barrier disruption induced by DSS, the presence of non-colonizing
421 microbes is associated with a more robust immune response than bacteria against which the host
422 has presumably been tolerized due to successful colonization and immune recognition. Immune
423 tolerance develops early in life when the host is first introduced to microbes. This first introduction
424 allows the immune system to develop a tolerance through development of Th2 response and
425 expansion of ROR γ ^t T helper lymphocytes and dendritic cells within the gut early in life³⁵. These
426 ROR γ ^t cell populations quickly decline soon after birth³⁶, and may explain the mild disease
427 severity in the ET and CF groups regardless of GM composition. The relatively mild disease
428 observed in the GM^{High}CH and GM^{High}GA groups suggests that tolerance is induced in adolescent
429 recipient mice, assuming there is successful colonization of the transferred GM.

430 Collectively, these findings suggest that administration of DSS and subsequent induction of
431 epithelial barrier defects can be used experimentally to assess colonization and immune
432 recognition of microbial exposures. Molecular methods may show evidence of microbial
433 exposures in the fecal DNA regardless of patent colonization. DSS-induced colitis provides a
434 disease phenotype driven by the immune response to the GM, including prior recognition of
435 antigens within the gut lumen.

436 The use of FMT to treat diseases including Crohn's disease, ulcerative colitis, and *Clostridioides*
437 *difficile* infection has been widely reported³⁷⁻³⁹. The use of a stool sample from a healthy donor to
438 restore a dysbiotic gut microbial community has shown great promise as a treatment. However,
439 there are instances in which FMT has been ineffective or even exacerbated IBD in patients⁴⁰⁻⁴².
440 Similarly, probiotics may be used to treat or prevent dysbiosis in IBD patients. The response to
441 probiotics can also be variable and clinical trials show that probiotics can exacerbate IBD
442 symptoms⁴³. The present data may provide a partial explanation for these adverse outcomes
443 following FMT or probiotic administration in IBD patients. In the context of disease-associated

444 epithelial damage, recognition of foreign antigens against which the host has not developed
445 tolerance may exacerbate disease.

446 Our study is not without its limitations. For the first experiment in this study, it was not possible to
447 truly determine the extent to which the co-housing donors transferred their microbiomes, as
448 weaning samples from the donors do not represent a fully developed GM of an adult and the
449 seven-week samples were collected after co-housing changed the donor microbiome by transfer
450 of microbes from the recipient mouse GM. However, as it has been shown that the dam will
451 efficiently transfer her GM to her pups soon after birth, the GM harbored by the dam of the CH
452 donor mice will be a sufficient representation of the donor GM. For the immunoassay, we only
453 measured 45 immune mediators, while we recognize that there are many more that can influence
454 disease severity. That said, well-characterized immune mediators were included in the assay,
455 both pro-inflammatory and anti-inflammatory. We also recognize that in performing weekly gastric
456 gavage, we introduced momentary acute stress by handling the mice. However, the goal of the
457 weekly gavage transfer was to eliminate physical contact and effects of social interaction.

458

459 **Conclusion**

460 In summary, our findings indicate that colonization efficiency following GM transfer is determined
461 by the relationship between donor and recipient GM, and that poor transfer efficiency is
462 associated with more severe disease. Moreover, these data provide further evidence that
463 methods used to manipulate the GM must be considered in the context of study reproducibility
464 when results between similar studies are not in agreement.

465

466 **Acknowledgments**

467 We would like to thank Dr. Rachel Olson, Dr. James Chung, and Amy Steeneck for their
468 knowledge and technical assistance with immune mediator concentration collection and analysis.
469 We would also like to thank Benjamin Olthoff for his technical assistance with DSS preparation
470 and administration, and Rebecca Dorfmeier for her assistance with fecal DNA sample
471 preparation for 16S rRNA amplicon sequencing analysis.

472

473 **Funding Statement**

474 KG, ZM, ACE, and CLF and project supplies and animals were supported by NIH U42 OD010918.
475 KG was also supported by NIH T32 OD011126 and the Joseph Wagner Fellowship Endowment
476 in Laboratory Animal Medicine and ZM was also supported by NIH T32 GM008396. TR was
477 supported by the University of Missouri Office of Research, Innovation and Impact, and the
478 Joseph Wagner Fellowship Endowment in Laboratory Animal Medicine.

479

480 **Disclosure statement**

481 The authors report there are no competing interests to declare.

482

483 **Data availability statement**

484 All 16S rRNA amplicon sequencing data are available at the NCBI Sequence Read Archive under
485 the BioProject number PRJNA1031529.

486

487 **References**

488

- 489 1 Afzaal, M. *et al.* Human gut microbiota in health and disease: Unveiling the relationship.
490 *Front Microbiol* **13**, 999001 (2022). <https://doi.org/10.3389/fmicb.2022.999001>
- 491 2 Hou, K. *et al.* Microbiota in health and diseases. *Signal Transduct Target Ther* **7**, 135
492 (2022). <https://doi.org/10.1038/s41392-022-00974-4>
- 493 3 Franzosa, E. A. *et al.* Gut microbiome structure and metabolic activity in inflammatory
494 bowel disease. *Nat Microbiol* **4**, 293-305 (2019).
- 495 4 Rebersek, M. Gut microbiome and its role in colorectal cancer. *BMC Cancer* **21**, 1325
496 (2021).
- 497 5 Taniya, M. A. *et al.* Role of Gut Microbiome in Autism Spectrum Disorder and Its
498 Therapeutic Regulation. *Front Cell Infect Microbiol* **12**, 915701 (2022).
- 499 6 Alam, M. T. *et al.* Microbial imbalance in inflammatory bowel disease patients at different
500 taxonomic levels. *Gut Pathog* **12**, 1 (2020). <https://doi.org/10.1186/s13099-019-0341-6>
- 501 7 Torres, J. *et al.* Infants born to mothers with IBD present with altered gut microbiome
502 that transfers abnormalities of the adaptive immune system to germ-free mice. *Gut* **69**,
503 42-51 (2020). <https://doi.org/10.1136/gutjnl-2018-317855>
- 504 8 Gevers, D. *et al.* The treatment-naïve microbiome in new-onset Crohn's disease. *Cell*
505 *Host Microbe* **15**, 382-392 (2014). <https://doi.org/10.1016/j.chom.2014.02.005>
- 506 9 McGuire, A. L. *et al.* Perspectives on human microbiome research ethics. *J Empir Res*
507 *Hum Res Ethics* **7**, 1-14 (2012).
- 508 10 Heijtz, R. D. *et al.* Normal gut microbiota modulates brain development and behavior.
509 *Proceedings of the National Academy of Sciences* **108**, 3047-3052 (2011).
510 <https://doi.org/10.1073/pnas.1010529108>
- 511 11 Nicholson, J. K. *et al.* Host-gut microbiota metabolic interactions. *Science* **336**, 1262-
512 1267 (2012). <https://doi.org/10.1126/science.1223813>
- 513 12 Tremaroli, V. & Bäckhed, F. Functional interactions between the gut microbiota and host
514 metabolism. *Nature* **489**, 242-249 (2012). <https://doi.org/10.1038/nature11552>
- 515 13 Dirnagl, U., Duda, G. N., Grainger, D. W., Reinke, P. & Roubenoff, R. Reproducibility,
516 relevance and reliability as barriers to efficient and credible biomedical technology
517 translation. *Adv Drug Deliv Rev* **182**, 114118 (2022).
518 <https://doi.org/10.1016/j.addr.2022.114118>
- 519 14 Pistollato, F. *et al.* Alzheimer's Disease, and Breast and Prostate Cancer Research:
520 Translational Failures and the Importance to Monitor Outputs and Impact of Funded
521 Research. *Animals (Basel)* **10** (2020). <https://doi.org/10.3390/ani10071194>
- 522 15 Collins, F. S. & Tabak, L. A. Policy: NIH plans to enhance reproducibility. *Nature* **505**,
523 612-613 (2014). <https://doi.org/10.1038/505612a>
- 524 16 Ericsson, A. C. *et al.* Supplier-origin mouse microbiomes significantly influence
525 locomotor and anxiety-related behavior, body morphology, and metabolism. *Commun*
526 *Biol* **4**, 716 (2021). <https://doi.org/10.1038/s42003-021-02249-0>
- 527 17 Tsou, A. M. *et al.* Utilizing a reductionist model to study host-microbe interactions in
528 intestinal inflammation. *Microbiome* **9**, 215 (2021). <https://doi.org/10.1186/s40168-021-01161-3>
- 529
- 530 18 Kimura, I. *et al.* Maternal gut microbiota in pregnancy influences offspring metabolic
531 phenotype in mice. *Science* **367** (2020). <https://doi.org/10.1126/science.aaw8429>
- 532 19 Schneider, K. M. *et al.* Imbalanced gut microbiota fuels hepatocellular carcinoma
533 development by shaping the hepatic inflammatory microenvironment. *Nat Commun* **13**,
534 3964 (2022). <https://doi.org/10.1038/s41467-022-31312-5>
- 535 20 Ericsson, A. C. *et al.* Effects of vendor and genetic background on the composition of the
536 fecal microbiota of inbred mice. *PLoS One* **10**, e0116704 (2015).
- 537 21 Long, L. L. *et al.* Shared and distinctive features of the gut microbiome of C57BL/6 mice
538 from different vendors and production sites, and in response to a new vivarium.

- 539 22 Zhang, C. *et al.* Transfer efficiency and impact on disease phenotype of differing
540 methods of gut microbiota transfer. *Sci Rep* **12**, 19621 (2022).
- 541 23 Hart, M. L. *et al.* Development of outbred CD1 mouse colonies with distinct standardized
542 gut microbiota profiles for use in complex microbiota targeted studies. *Sci Rep* **8**, 10107
543 (2018).
- 544 24 Hart, M. L. *et al.* Development of outbred CD1 mouse colonies with distinct standardized
545 gut microbiota profiles for use in complex microbiota targeted studies. *Scientific Reports*
546 **8** (2018). <https://doi.org/10.1038/s41598-018-28448-0>
- 547 25 Mahabir, E. *et al.* Reproductive Performance after Unilateral or Bilateral Oviduct Transfer
548 of 2-Cell Embryos in Mice. *J Am Assoc Lab Anim Sci* **57**, 110-114 (2018).
- 549 26 Walters, W. A. *et al.* PrimerProspector: de novo design and taxonomic analysis of
550 barcoded polymerase chain reaction primers. *Bioinformatics* **27**, 1159-1161 (2011).
551 <https://doi.org/10.1093/bioinformatics/btr087>
- 552 27 Caporaso, J. G. *et al.* Global patterns of 16S rRNA diversity at a depth of millions of
553 sequences per sample. *Proc. Natl. Acad. Sci. U.S.A.* **108 Suppl 1**, 4516-4522 (2011).
554 <https://doi.org/10.1073/pnas.1000080107>
- 555 28 Loy, A., Maixner, F., Wagner, M. & Horn, M. probeBase--an online resource for rRNA-
556 targeted oligonucleotide probes: new features 2007. *Nucleic Acids Res* **35**, D800-804
557 (2007). <https://doi.org/10.1093/nar/gkl856>
- 558 29 Martin, M. Cutadapt removes adapter sequences from high-throughput sequencing
559 reads. *EMBnet.journal* **17**, 10-12 (2011).
560 <https://doi.org/https://doi.org/10.14806/ej.17.1.200>.
- 561 30 Bolyen, E. *et al.* Reproducible, interactive, scalable and extensible microbiome data
562 science using QIIME 2. *Nat Biotechnol* **37**, 852-857 (2019).
563 <https://doi.org/10.1038/s41587-019-0209-9>
- 564 31 Callahan, B. J. *et al.* DADA2: High-resolution sample inference from Illumina amplicon
565 data. *Nat Methods* **13**, 581-583 (2016). <https://doi.org/10.1038/nmeth.3869>
- 566 32 Hammer, Ø. & Harper, D. A. Past: paleontological statistics software package for
567 education and data analysis. *Palaeontologia electronica* **4**, 1 (2001).
- 568 33 Dixon, P. VEGAN, A Package of R Functions for Community Ecology. *Journal of*
569 *Vegetation Science* **14**, 927-930 (2003).
- 570 34 Bittinger, K. usedist: Distance matrix utilities. *R package version 0.4. 0* (2020).
- 571 35 Ohnmacht, C. *et al.* The microbiota regulates type 2 immunity through ROR γ ⁺ T cells.
572 *Science* **349**, 989-993 (2015).
- 573 36 Akagbosu, B. *et al.* Novel antigen-presenting cell imparts Treg-dependent tolerance to
574 gut microbiota. *Nature* **610**, 752-760 (2022).
- 575 37 Kelly, C. R. *et al.* Fecal Microbiota Transplantation Is Highly Effective in Real-World
576 Practice: Initial Results From the FMT National Registry. *Gastroenterology* **160**, 183-192
577 e183 (2021). <https://doi.org/10.1053/j.gastro.2020.09.038>
- 578 38 Lopez, J. & Grinspan, A. Fecal Microbiota Transplantation for Inflammatory Bowel
579 Disease. *Gastroenterol Hepatol (N Y)* **12**, 374-379 (2016).
- 580 39 van Nood, E. *et al.* Duodenal infusion of donor feces for recurrent *Clostridium difficile*. *N*
581 *Engl J Med* **368**, 407-415 (2013). <https://doi.org/10.1056/NEJMoa1205037>
- 582 40 Khoruts, A. *et al.* Inflammatory Bowel Disease Affects the Outcome of Fecal Microbiota
583 Transplantation for Recurrent *Clostridium difficile* Infection. *Clin Gastroenterol Hepatol*
584 **14**, 1433-1438 (2016). <https://doi.org/10.1016/j.cgh.2016.02.018>
- 585 41 Fischer, M. *et al.* Fecal Microbiota Transplantation is Safe and Efficacious for Recurrent
586 or Refractory *Clostridium difficile* Infection in Patients with Inflammatory Bowel Disease.
587 *Inflamm Bowel Dis* **22**, 2402-2409 (2016).
588 <https://doi.org/10.1097/MIB.0000000000000908>

- 589 42 Chin, S. M. *et al.* Fecal Microbiota Transplantation for Recurrent *Clostridium difficile*
590 Infection in Patients With Inflammatory Bowel Disease: A Single-Center Experience. *Clin*
591 *Gastroenterol Hepatol* **15**, 597-599 (2017). <https://doi.org/10.1016/j.cgh.2016.11.028>
592 43 Dore, M. P., Bibbo, S., Fresi, G., Bassotti, G. & Pes, G. M. Side Effects Associated with
593 Probiotic Use in Adult Patients with Inflammatory Bowel Disease: A Systematic Review
594 and Meta-Analysis of Randomized Controlled Trials. *Nutrients* **11** (2019).
595 <https://doi.org/10.3390/nu11122913>

596

597 **Figure Legends**

598 **Figure 1.** Characterization and comparison of the six transfer groups to determine efficiency of
599 GM transfer. Principal coordinate analysis comparing the three transfer methods of the (a) GM^{High}
600 and the (b) GM^{Low} group's beta diversity to their donors. X and Y axes labeled with percent of
601 variation contributed by Principal coordinate 1 (PCo1) and PCo2, respectively. Two-way
602 PERMANOVA for main effects of transfer method and recipient/donor (**Sup Table S2**), followed
603 by a one-way PERMANOVA to test pairwise comparisons between donor and recipient (**Sup**
604 **Table S3**). Comparison of donor and recipient GM at seven weeks of age for the (c) GM^{High} and
605 (d) GM^{Low} cohorts. Bars represent mean chao-1 richness +/- SD. Two-way ANOVA for main
606 effects of transfer method and sex. **ns** - not significant, **** p<0.0001.

607 **Figure 2.** Comparison DSS-colitis disease phenotype differences of the six transfer groups. (a)
608 Comparison of the DSS-induced weight loss between the GM^{High} cohort transfer methods. One-
609 way ANOVA for effect of transfer method (p = 0.013, F = 4.5). Tukey *post hoc* for pairwise
610 comparisons. (b) Comparison of the DSS-induced weight loss between the GM^{Low} cohort transfer
611 methods. Kruskal-Wallis ANOVA on ranks for effect of transfer method (p <0.0001, F = 51.4).
612 Dunn's *post hoc* for pairwise comparisons. Each data point in panels (a) and (b) represents
613 transfer method mean percent weight change +/- SEM. DSS-induced disease survivability of the
614 (c) GM^{High} cohorts and the (d) GM^{Low} cohorts. Cox proportional hazards for main effects of transfer
615 method and sex. (e) Colon lengths for each cohort following DSS administration and (f) DSS-
616 induced lesion scores for each cohort. Groups that differ in letter designation are statistically

617 significant from each other, while groups that share the same letter designation are not statistically
618 significant from each other. Three Way ANOVA for main effects of transfer method, transfer
619 direction, and sex. **ns** - not signification, **** p<0.0001.

620 **Figure 3.** Comparison of co-housing and gavage GM transfer efficiency and DSS-induced DSS
621 phenotype in each transfer direction. **(a)** PCoA comparing the GM beta diversity of the CH and
622 GA cohorts in each transfer direction. X and Y axes labeled with percent of variation contributed
623 by PCo1 and PCo2, respectively. Two-way PERMANOVA for main effects of transfer method and
624 transfer direction. **(b)** Chao-1 richness of each co-housing and gavage cohorts. Three-way
625 ANOVA for main effects of transfer method, transfer direction, and sex. **(c)** DSS-induced weight
626 loss comparison of the co-housing and gavage cohorts. Each point represents group mean
627 percent weight change +/- SEM. Two-way ANOVA for main effects of transfer method and transfer
628 direction. **(d)** DSS-induced disease survivability of the co-housing and gavage cohorts. Cox
629 proportional hazards for main effects of transfer method, transfer direction, and sex. **(e)** Colon
630 lengths and **(f)** histological lesion scores caused by DSS-induced colitis. Three-way ANOVA for
631 main effects of transfer method, transfer direction, and sex. **p<0.01, ***p<0.001, ****p<0.0001.

632 **Figure 4.** Immune mediator concentrations from the co-housing and gavage cohorts' colons
633 following DSS-induced colitis. Volcano plots comparing the cytokine and chemokine
634 concentrations between **(a)** GM^{High} and GM^{Low} cohorts, and **(b)** gavage and co-housing cohorts.
635 Immune mediator concentration comparison of the co-housing and gavage cohorts for **(c)**
636 macrophage inflammatory protein 2-alpha (MIP-2 α), **(d)** interleukin 22 (IL-22), and **(e)** interleukin 6
637 (IL-6). Bars represent mean immune mediator concentrations +/- SD. Three-way ANOVA for main
638 effects of transfer method, transfer direction, and sex. *p<0.05, **p<0.01, ***p<0.001.

639

640 **Supplemental Figure Legends**

641 **Sup Fig S1.** Schematic of the generation of each GM transfer cohort used in the study. **(a)** 2-cell
642 stage embryos were collected from B6J mice and implanted into pseudopregnant CD-1 mice
643 harboring GM^{High}. **(b)** 2-cell stage embryos were collected from B6N mice and implanted into
644 pseudopregnant CD-1 mice harboring GM^{Low}. **(c)** Pups of less than 24-hours were cross-fostered
645 from B6J dams onto a CD-1 dam harboring GM^{High}. **(d)** Pups of less than 24-hours were cross-
646 fostered from B6N dams onto a CD-1 dam harboring GM^{Low}. **(e)** B6J mice were weaned into cages
647 with weaned CD-1 donor mice harboring GM^{High} so that the CD-1 donors would transfer their
648 GM^{High} via coprophagia to the B6J mice. **(f)** B6N mice were weaned into cages with weaned CD-
649 1 donors harboring GM^{Low} so that the CD-1 mice would transfer their GM^{Low} via coprophagia to
650 the B6N mice. **(g)** Similar to experiment 1, B6J mice were weaned into cages with weaned CD-1
651 donor mice harboring GM^{High} so that the CD-1 donors would transfer their GM^{High} via coprophagia
652 to the B6J mice. **(h)** Similar to experiment 1, B6N mice were weaned into cages with weaned CD-
653 1 donors mice harboring GM^{Low} so that the CD-1 donors would transfer their GM^{Low} via
654 coprophagia to the B6N mice. **(i)** B6J mice were gastric gavaged with fecal material from GM^{High}
655 donors beginning at weaning and exposed to GM^{High} via dirty bedding transfer from cages housing
656 the GM^{High} CD-1 GM donors to allow GM transfer via coprophagia. **(j)** B6N mice were gastric
657 gavaged with fecal material from GM^{Low} donors beginning at weaning and exposed to GM^{Low} via
658 dirty bedding transfer from cages housing the GM^{Low} CD-1 GM donors to allow GM transfer via
659 coprophagia. For clarity, the white CD-1 mice in the schematic are the GM donors, and the
660 recipient mice are the black B6 mice to the right of the CD-1 donors.

661 **Sup Fig S2.** PCoA comparing the six treatment groups' GM beta diversity to the beta diversity of
662 the donors. X and Y axes labeled with percent of variation contributed by Principal coordinate 1
663 (PCo1) and PCo2, respectively. Three-way PERMANOVA for main effects of transfer method,
664 transfer direction, and donor/recipient (**Sup Table S2**), followed by a one-way PERMANOVA to
665 test pairwise comparisons between donor and recipient (**Sup Table S3**).

666 **Sup Fig S3.** Weaning and week seven weights of the six ET, CF, and CH cohorts. Weaning
667 weights collected from the three (a) GM^{High} cohorts and the three (b) GM^{Low} cohorts. Weights
668 collected at seven weeks of age prior to DSS administration of the three (c) GM^{High} cohorts and
669 the three (d) GM^{Low} cohorts. Two-way ANOVA for main effects of transfer direction and sex.
670 *p<0.05, ****p<0.0001.

671 **Sup Fig S4.** Comparison of the GM^{High}CH and GM^{Low}CH weight loss and disease survivability
672 phenotypes. (a) DSS-induced weight loss comparison of the two co-housing cohorts. Each data
673 point represents group mean percent weight change +/- SEM. Students t-test. (b) DSS-induced
674 disease survivability of each co-housing cohort. Survival LogRank. ****p<0.0001.

675 **Sup Fig S5.** Colon length is not determined by day of DSS-induced colitis treatment at which
676 animals needed to be euthanized, but histological lesion score is dependent on day of DSS
677 treatment in the GM^{Low}CH cohort. (a) Comparison of the day that animals need to be euthanized
678 due to weight loss (denoted by color), and the length of colons measured at time of necropsy. (b)
679 Comparison of the day that animals need to be euthanized due to weight loss (denoted by color),
680 and histological lesion score of the colons.

681 **Sup Fig S6.** The pattern of transferring the GM at time of weaning leading to a decreased
682 efficiency of transfer is repeatable. (a) Principal coordinates analysis comparing the GM^{High} and
683 GM^{Low}CH and GA groups to their donor GMs. X and Y axes labeled with percent of variation
684 contributed by PCo1 and PCo2, respectively. Two-way PERMANOVA for main effects of transfer
685 method and group (**Sup Table S7**), followed by a one-way PERMANOVA to test pairwise
686 comparisons between respective donors and recipients (**Sup Table S8**). Chao-1 richness of the
687 (b) GM^{High} CH and GA cohorts to the GM^{High} donors, and the (c) GM^{Low} CH and GA cohorts to the
688 GM^{Low} donors. Two-way ANOVA for main effects of transfer method and donor/recipient. **ns** - not
689 significant, * p<0.05, ** p<0.01, **** p<0.0001. For the **Sup Fig S6 figures**, we chose to use the
690 GA donors from both transfer directions to represent the GM the recipients should have received

691 (Both CH and GA) as the CH donors' GM was modified by the recipients' GM during co-housing
692 and is therefore not a proper representation of the GM alpha- and beta-diversity we wanted the
693 recipients to receive. The GA CD-1 donors were housed separate of their recipients and were not
694 exposed to the GMs of the B6J or B6N mice, and thus were a better representation of what the
695 recipients' GM should look like if GM transfer was successful. For statistical purposes, the main
696 effect of group in the two-way ANOVA consisted of the donor group compared with the CH and
697 GA recipients pooled as one group within transfer direction. We used a one-way PERMANOVA
698 for individual pairwise comparisons of the beta diversity between the GA donors and CH and GA
699 recipients, and one-way ANOVA to compare richness of the GA donors to the CH and GA
700 recipients.

701

702 **Supplemental Table Legends**

703 **Sup Table S1.** Histological lesion scoring criteria used to assign lesion score to DSS treated
704 colons.

705 **Sup Table S2.** Results of three-way PERMANOVA comparing beta-diversity of ET, CF, and CH
706 groups and the donors, with main effects including transfer method, transfer direction, and
707 donor/recipient.

708 **Sup Table S3.** Results of one-way PERMANOVA pairwise comparisons of the six ET, CF, and
709 CH recipients and their respective donors. Jaccard dissimilarity distances were measured from
710 recipient group centroid to the centroid of the respective donor group.

711 **Sup Table S4.** Immune mediatory group averages and results of Mann-Whitney U Test between
712 GM^{High} and GM^{Low} cohorts for immune mediator concentrations.

713 **Sup Table S5.** Immune mediator group averages and results of Mann-Whitney U Test between
714 co-housing and gavage cohorts for immune mediator concentrations analyzed.

715 **Sup Table S6.** Cohort means and standard deviations for all immune mediators analyzed.

716 **Sup Table S7.** Results of the two-way PERMANOVA comparing beta-diversity of CH and GA
717 cohorts to their respective donors, with main effects including transfer method and
718 donor/recipient.

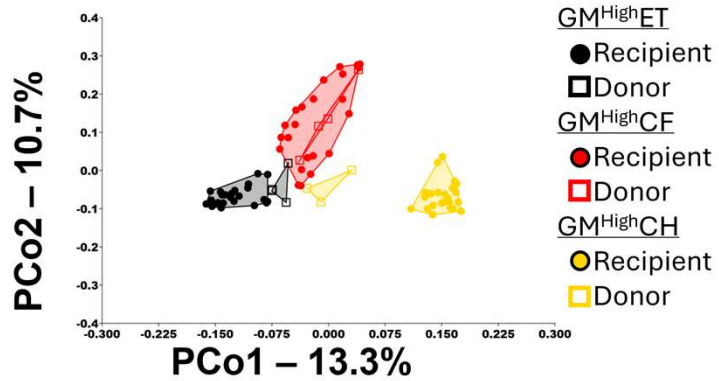
719 **Sup Table S8.** Results of one-way PERMANOVA pairwise comparisons of the CH and GA
720 cohorts beta diversity with their respective donors.

High Richness Donor (D) ➔ Low Richness Recipient (R)

Low Richness Donor (D) ➔ High Richness Recipient (R)

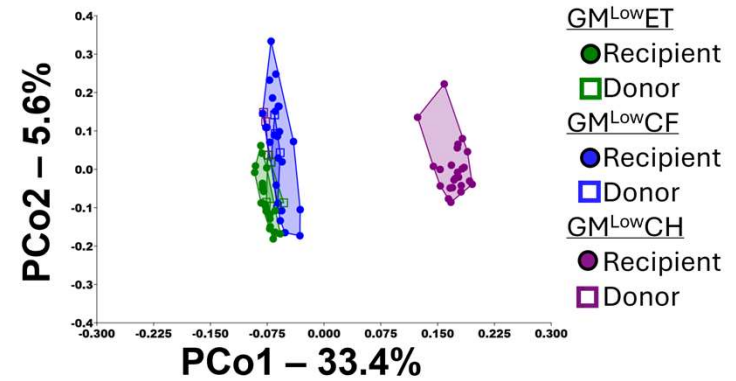
a Two-Way PERMANOVA

Transfer Method: P = 0.0001 F = 10.6
 Donor/Recipient: P = 0.0005 F = 2.4
 Interaction: P = 0.0001 F = 1.9

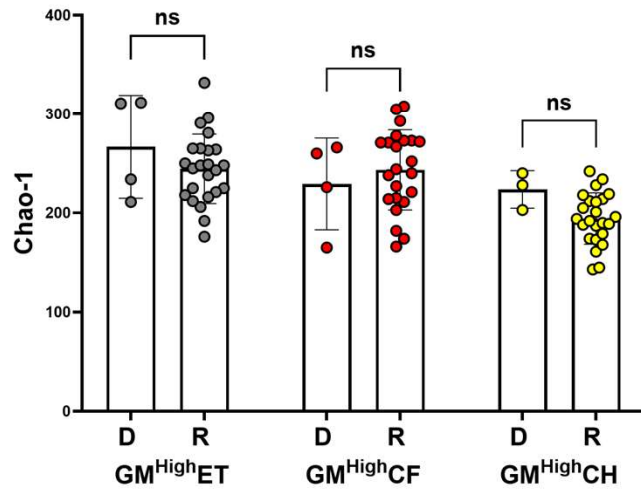


b Two-Way PERMANOVA

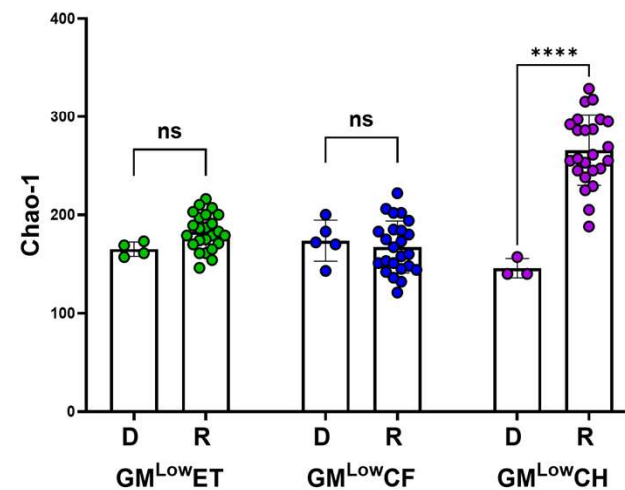
Transfer Method: P = 0.0001 F = 21.1
 Donor/Recipient: P = 0.0006 F = 5.5
 Interaction: P = 0.0001 F = 3.6



c

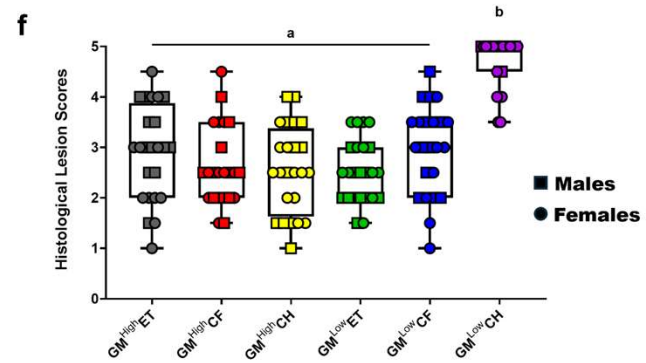
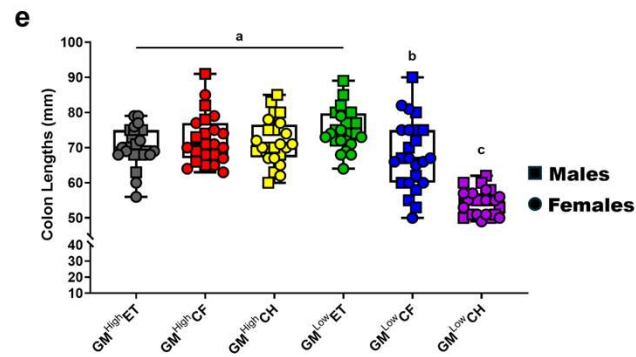
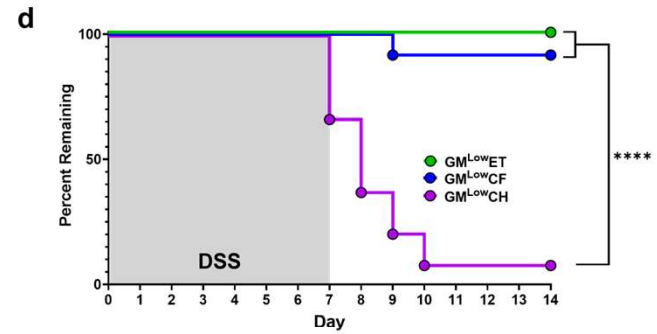
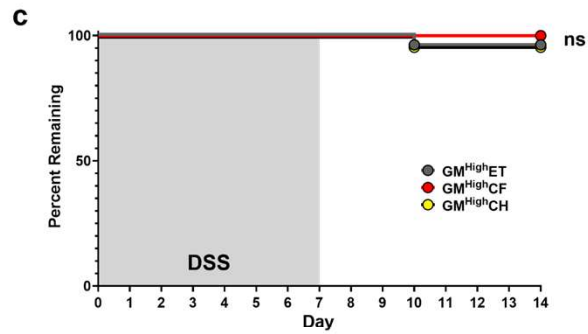
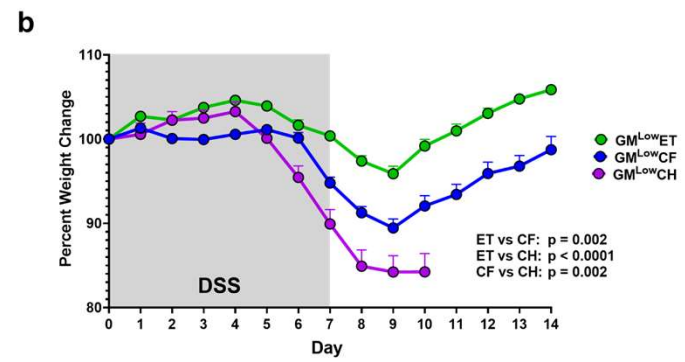
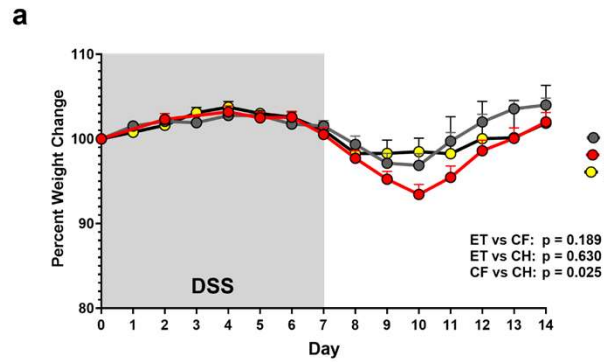


d

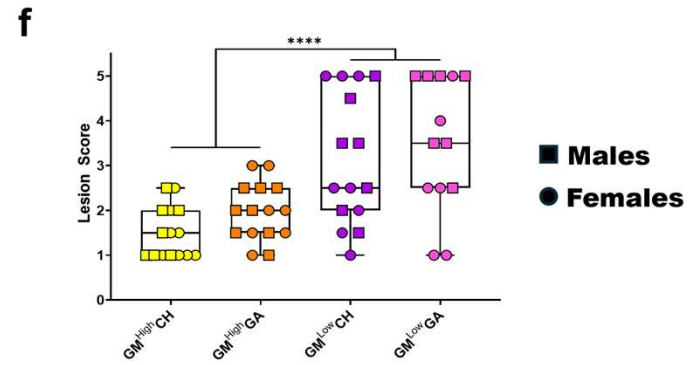
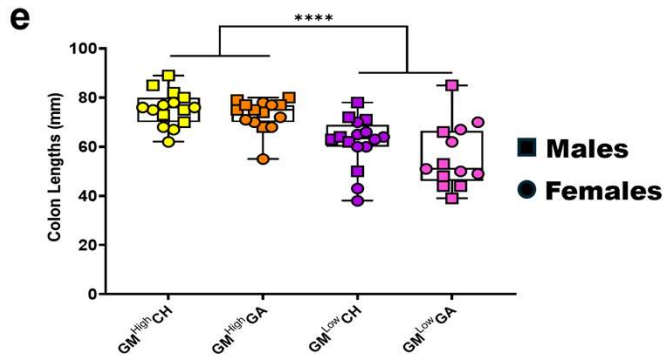
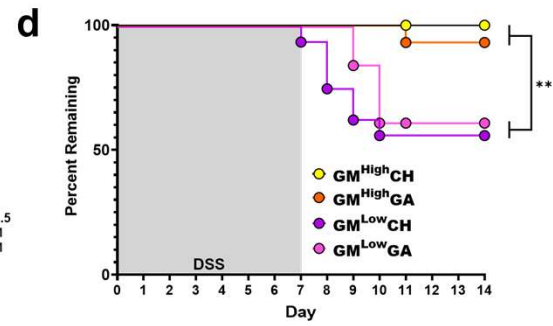
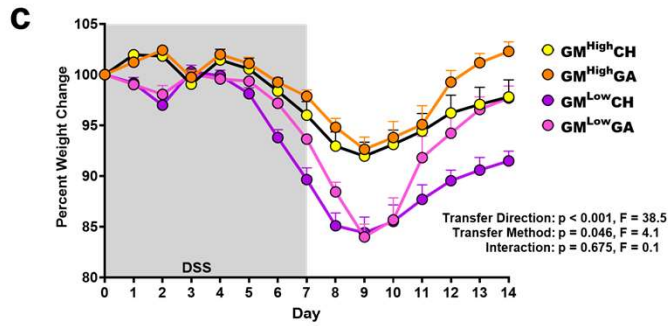
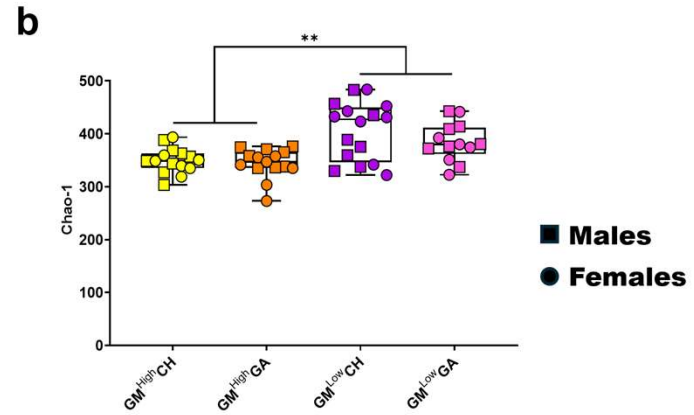
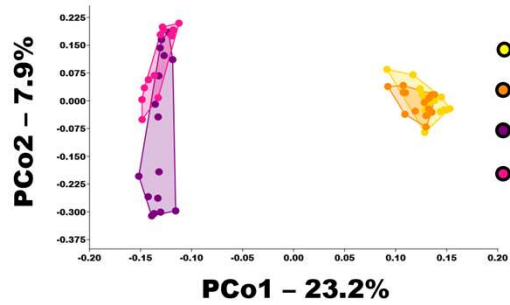


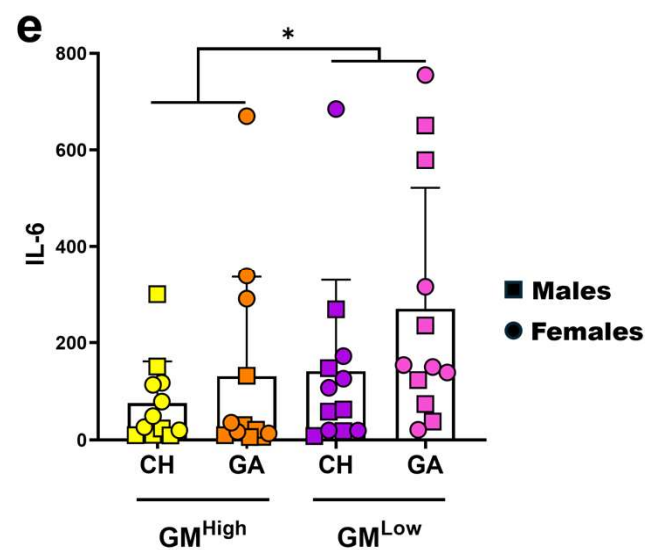
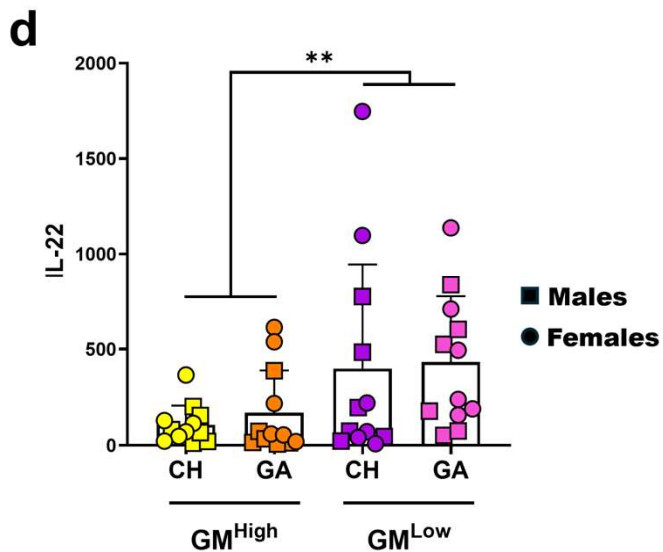
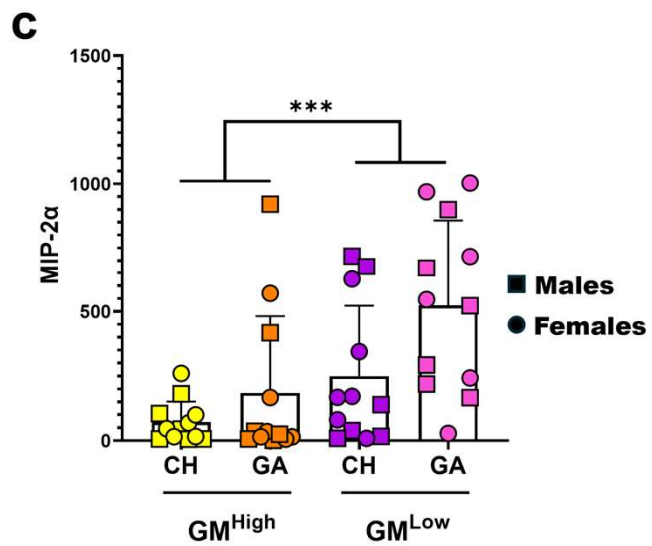
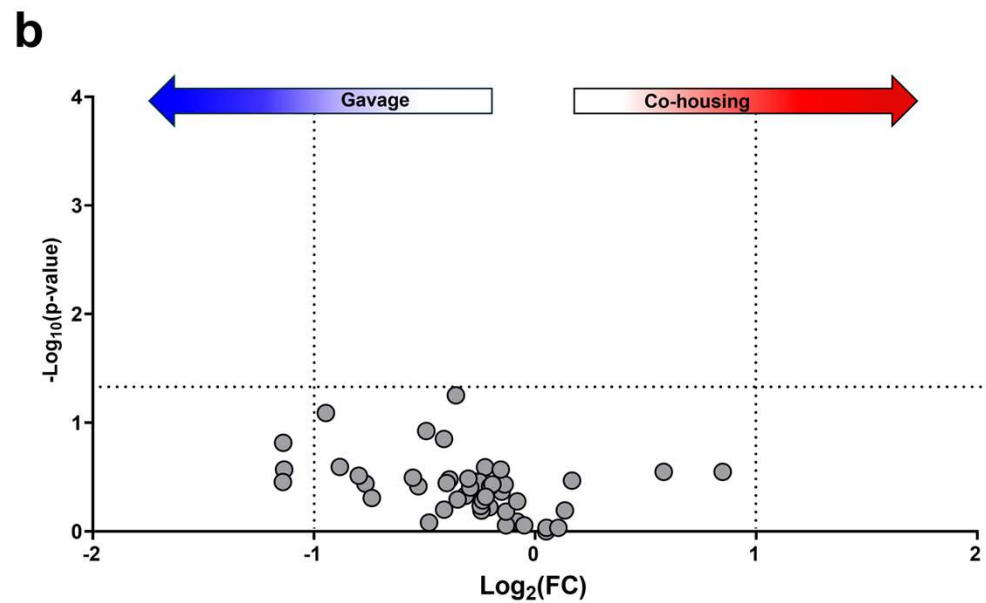
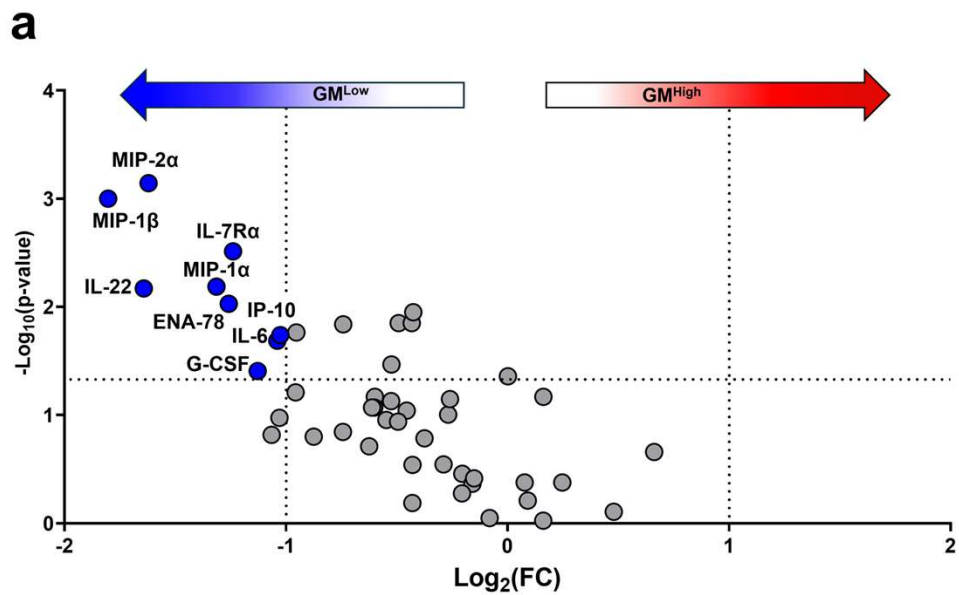
High Richness Donor (D) → Low Richness Recipient (R)

Low Richness Donor (D) → High Richness Recipient (R)

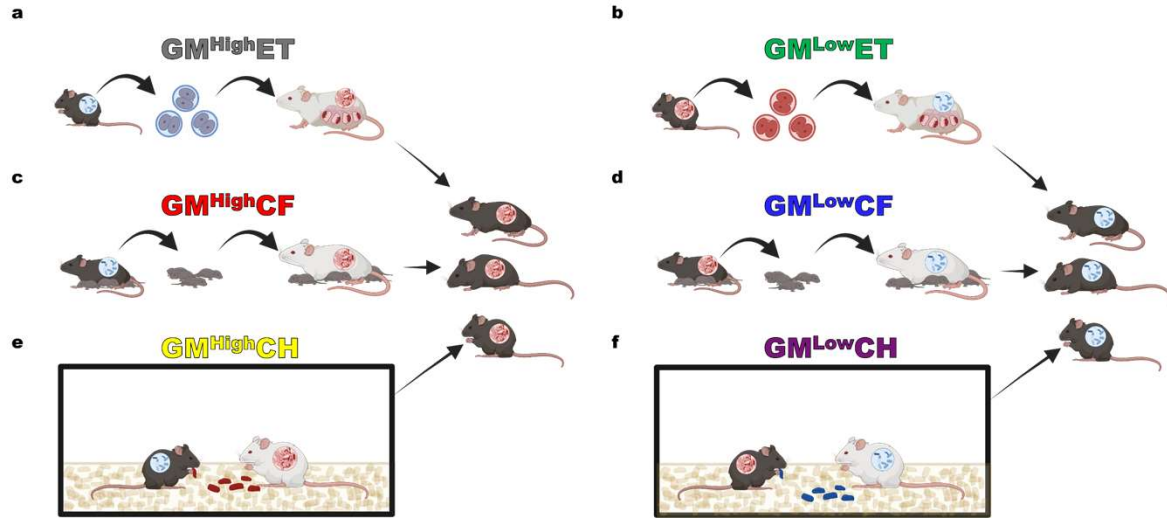


a Two-Way PERMANOVA
 Transfer Method: P = 0.0004 F = 3.7
 Transfer Direction: P = 0.0001 F = 18.9
 Interaction: P = 0.0007 F = 3.5

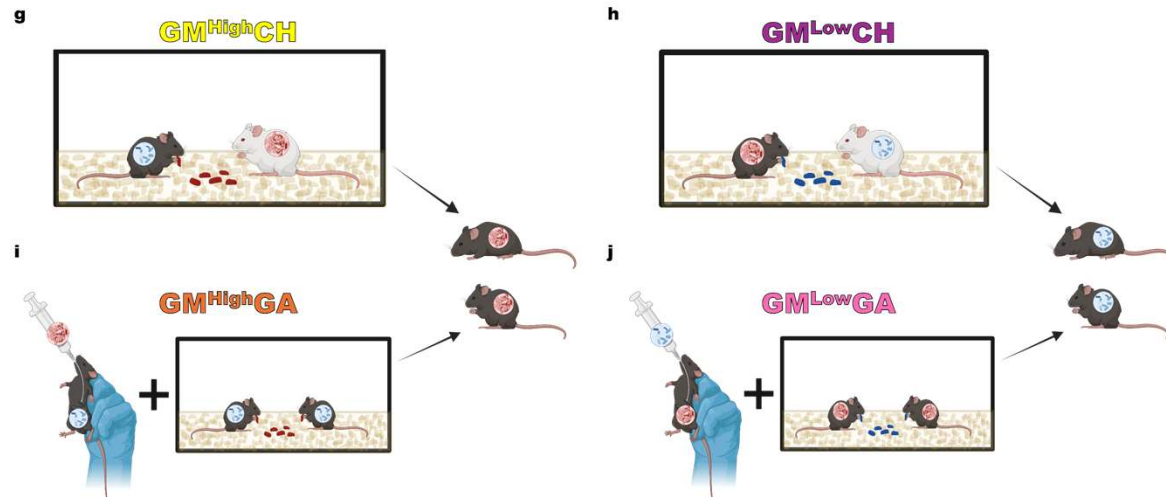


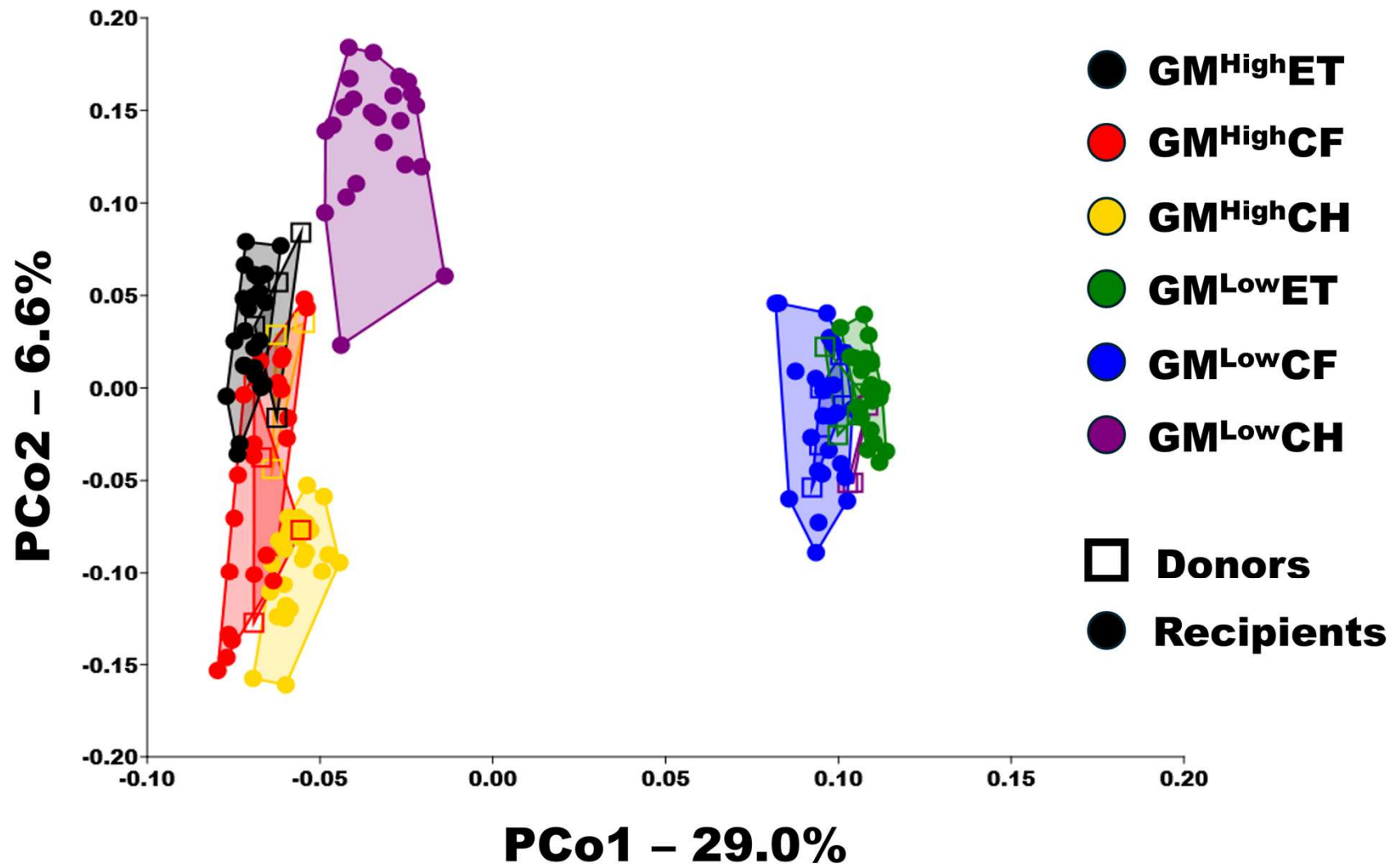


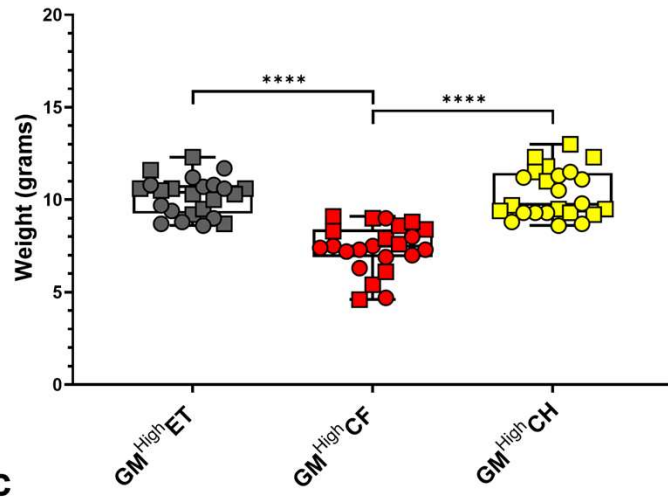
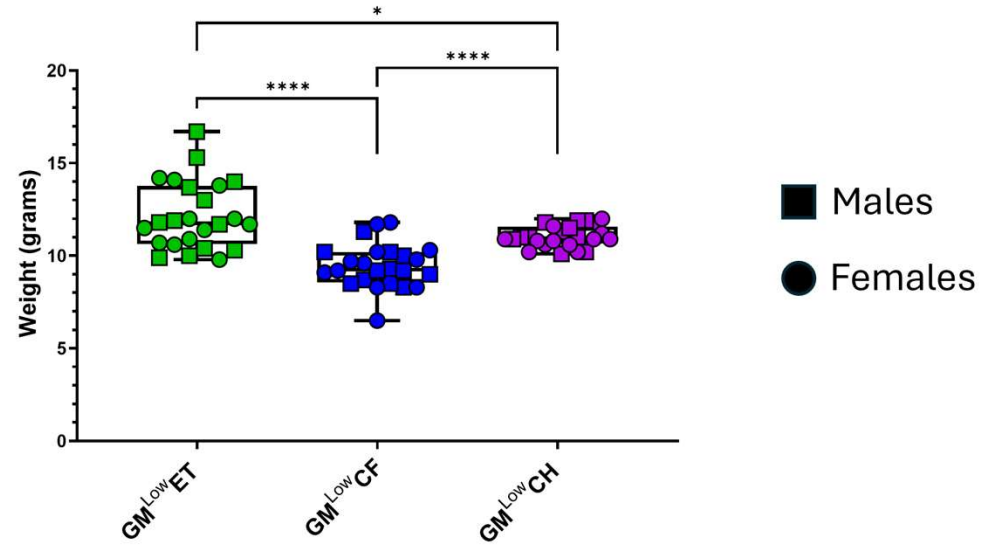
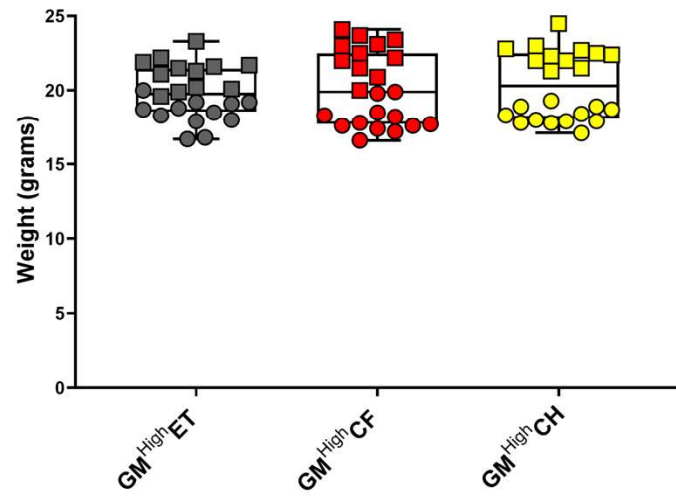
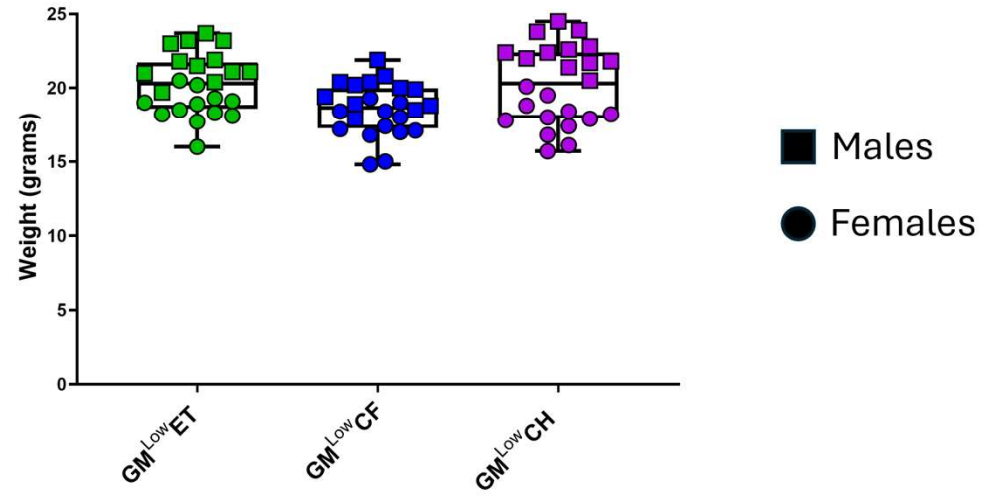
Experiment 1

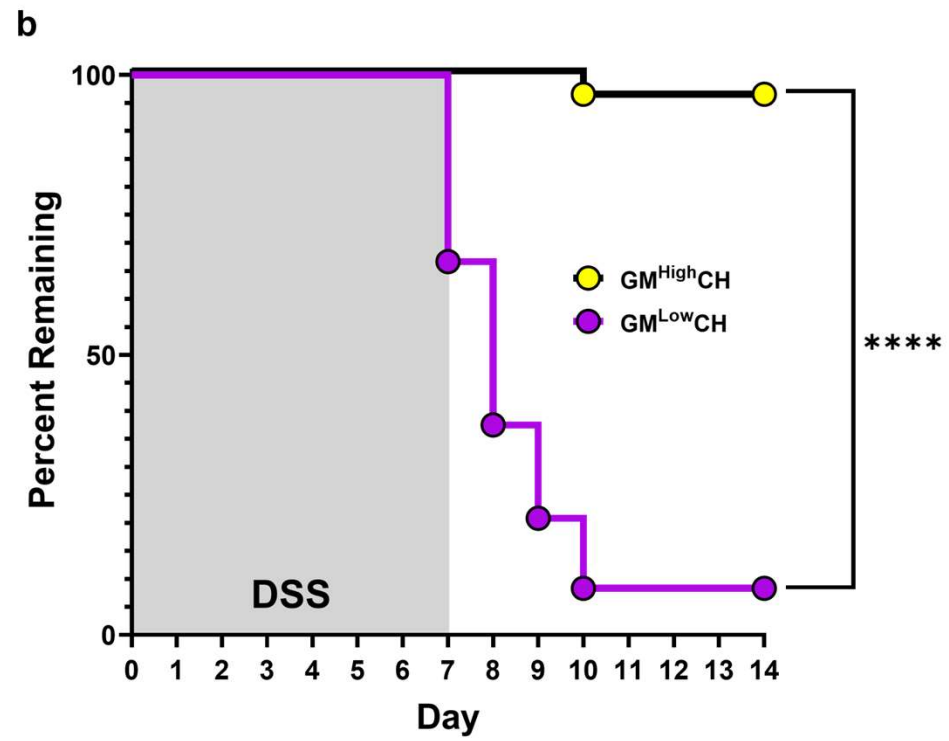
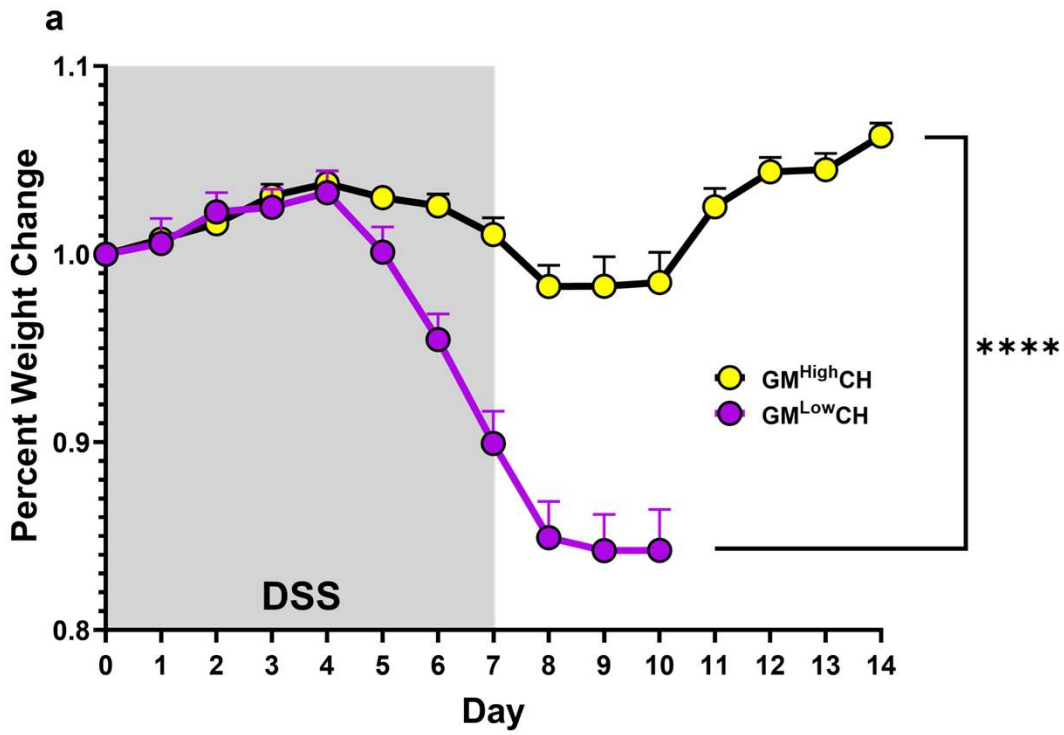


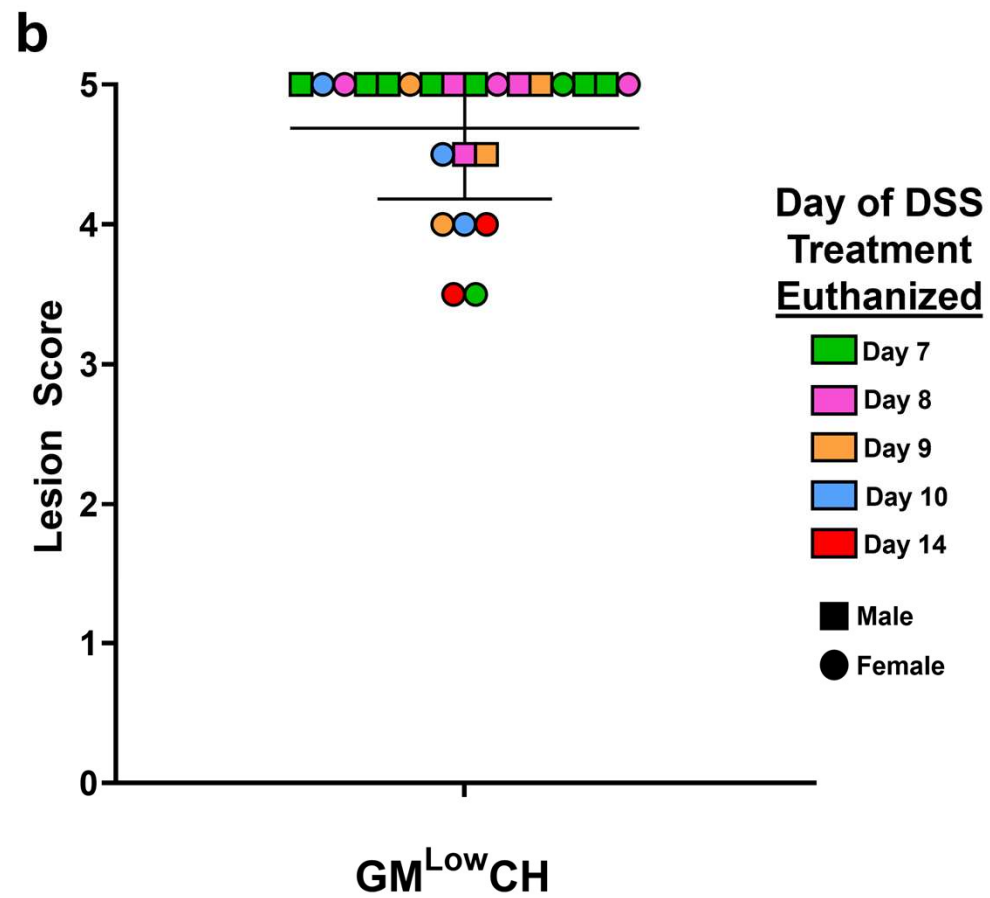
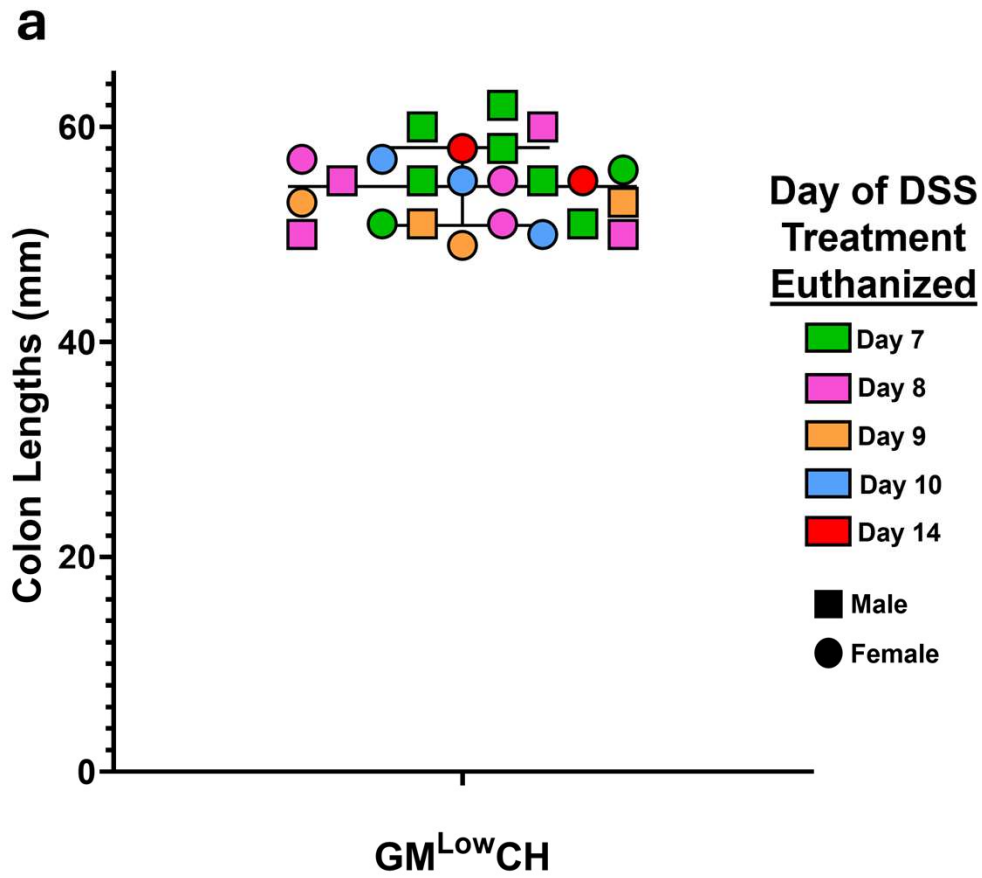
Experiment 2

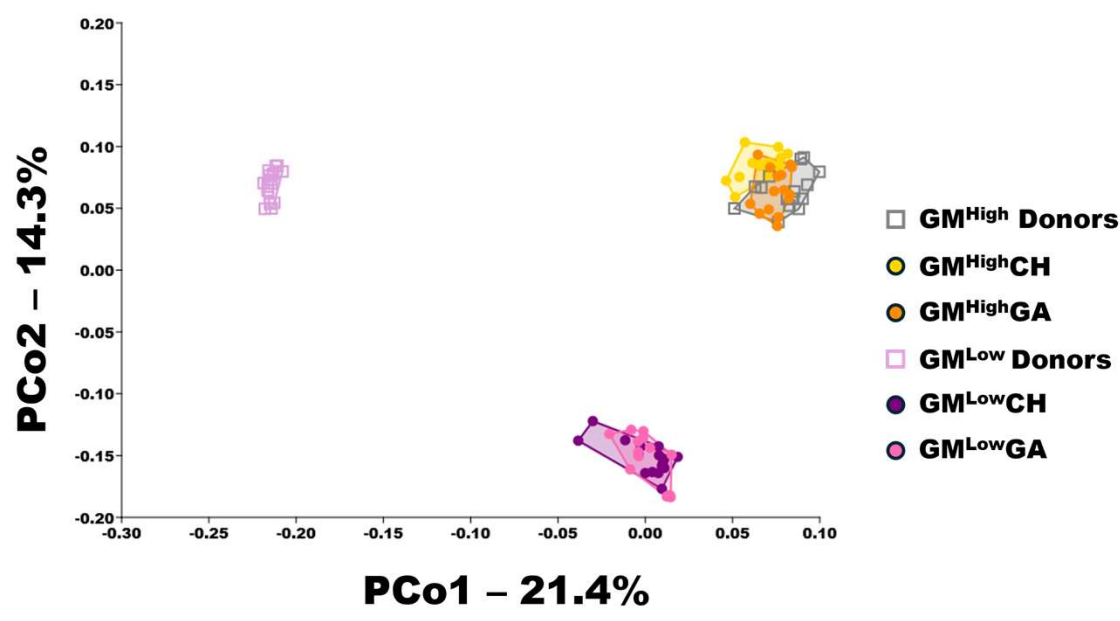
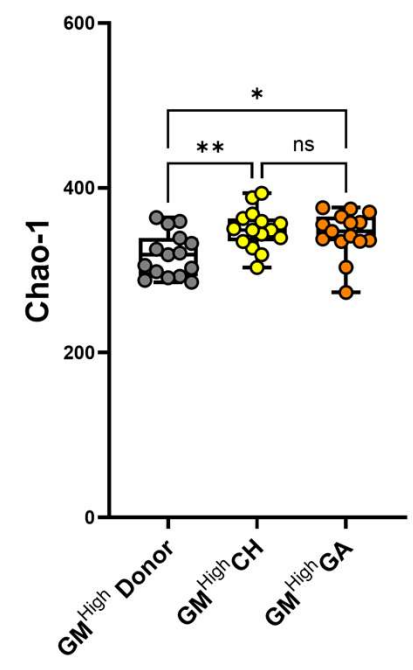




a**b****c****d**





a**b****c**